

Pore Water Pressure Influence on Geosynthetic Stabilized Subgrade Performance

B.R. Christopher, Ph.D., P.E., Christopher Consultants, Roswell, Georgia, USA
S.W. Perkins, Ph.D., P.E., Montana State University, Bozeman, Montana, USA
B.A. Lacina, P.E., TenCate Geosynthetics, Pendergrass, Pendergrass, Georgia, USA
W.A. Marr, Ph.D., P.E., Geocomp Corporation, Boxborough, MA, USA

ABSTRACT

Surfaced and unsurfaced roadways underlain by weak subgrade typically experience distress in the form of rutting. Geosynthetics are commonly used for base reinforcement and subgrade stabilization to reduce rutting, thereby improving roadway performance. Weak subgrades are typically wet, nearly saturated fine-grained soils. Traffic loads produce a pore pressure increase in the subgrade that grows with traffic repetitions. Development of pore pressure reduces the effective stress in the subgrade and thereby reduces the subgrade stiffness and strength. The reduction of stiffness and strength can have a dramatic impact on the performance of the roadway as expressed in terms of rutting. The purpose of this paper is to display results from pavement box test sections where a weak, nearly saturated subgrade was used and instrumented with pore pressure transducers. The results show a significant increase in pore water pressure, which is influenced by the type of geosynthetic used for base reinforcement and/or stabilization. In most cases, the pore pressure developed was found to directly correspond to the surface deformation measurements in terms of both the rate and magnitude of rutting. Results from mechanistic-modeling are shown to illustrate how the effect of pore pressure might be accounted for in existing pavement modeling principles.

1. INTRODUCTION

Most of the current empirical design models for geosynthetics in roadway stabilization are based on bearing capacity theory with modifications for inclusion of the geosynthetic (e.g., Barenberg, 1975; Steward et al., 1977; Giroud and Noiray, 1981; and, Giroud and Han, 2004). In each of those methods, the subgrade soil is assumed to be saturated and exhibit undrained behavior under traffic loading. The design charts or the input values to computer programs contain a property of the subgrade (resilient modulus, undrained shear strength and/or CBR). This property represents a measure of the in-place subgrade prior to construction or trafficking of the roadway. However, field measurements of this property are likely to be made on partially saturated soil in a pre-trafficking condition. Thus, this initial value of stiffness or strength may not be the same after roadway construction or trafficking, as the soil could change in volume and thus water content due to compression. In addition, the soil may become saturated, again due to compression, and develop pore water pressure during repeated loadings, which will result in a reduction of subgrade stiffness/strength. The development of pore water pressure can thus occur in both saturated and unsaturated soil, but is most likely more pronounced in a saturated soil. As a result, the deformation response measured in the field or in full scale lab models may not match the design charts as has been reported in the literature (e.g., see Christopher et al., 2001). Measurement of excess pore water pressure during trafficking can be used to adjust and more accurately model the strength of the soil during trafficking.

In full scale box tests performed to evaluate geosynthetics used in both stabilization and base reinforcement, the authors have observed the development and increase in pore water pressure during cyclic loading (Perkins et al., 2004; Christopher and Lacina, 2008; Christopher and Perkins, 2008). As indicated in these references, the pore water pressure measurements in most of the tests were found to directly correspond to the performance of the geosynthetic with the largest amount of deformation per cycle occurring in the tests with the highest developed pore pressure (e.g., the control tests) and the best performing tests (least amount of rutting under the same number of cycles) showing the lowest amount of pore pressure. These results indicate that the performance of the geosynthetics vary with both the subgrade type and conditions (i.e., a geosynthetic may perform well in one condition and not so well under other conditions). Geosynthetics could influence the development and magnitude of pore water pressure through: 1) a reduction in stress in the subgrade (Berg et al., 2000); 2) separation, which would reduce point stress and corresponding pore pressure developed from gravel penetration into subgrade layers (Christopher and Lacina, 2008); and/or, 3) pore pressure dissipation in the plane of some geosynthetics when the in plane permeability is greater than the permeability of the base layer (e.g., poorly draining base layers containing fine grained soils) (Holtz et al., 2008).

In this paper, an example of pore water pressure developed during stabilization tests with and without geosynthetics is presented. Effective stress principles are then used to evaluate the influence of the pore pressure on the strength of the soil. The strength of the soil is then incorporated into a design model using mechanistic modeling to illustrating how the effect of pore pressure might be accounted for in design using existing pavement modeling principles.

2. EXAMPLE OF PORE WATER PRESSURE INFLUENCE ON STABILIZATION PERFORMANCE

Figure 1 shows example results from full scale laboratory stabilization tests with and without a geosynthetic. Figure 1a shows the response to cyclic loading in terms of the permanent surface deformation plotted against number of load cycles to log scale. Figure 1b shows the dynamic deformation plotted against log of load cycle and Figure 1c gives the excess pore pressure in the upper portion of the subgrade beneath the load plate as reported by Perkins et al., 2008. The geosynthetic was a polypropylene fibrillated filament woven geotextile, GT_{w-f} . The subgrade soil was brown sandy silt (ML-MH). The subgrade has a standard Proctor maximum dry unit weight of 97 lb/ft^3 and an optimum moisture content of 22 %. The material was placed at a moisture content of approximately 36 %, which produced an in-place CBR of 1. Vane shear tests on in-place material produced a strength of 30 kPa (620 psf) in both sections. The in-place unit dry weight and moisture content was approximately 85 lb/ft^3 and 36 %, respectively. The base course aggregate was a graded aggregate meeting the Georgia Department of Transportation specifications. The material has a maximum dry unit weight of 145 lb/ft^3 , an optimum moisture content of 5.4 %, and a drained friction angle of 43 degrees. The material was placed at a moisture content of 6 % and at an average dry unit weight of 136 lb/ft^3 . The complete details of the test program are reported by Christopher and Lacina, 2008. As can be seen from Figure 1c, the pore water pressure measured in the control test section was significantly higher than in the geotextile test section. These measurements indicate that strength of the soil, although the same in both sections at the beginning of the test, was reduced during repeated loading, with a much greater strength loss occurring in the control section.

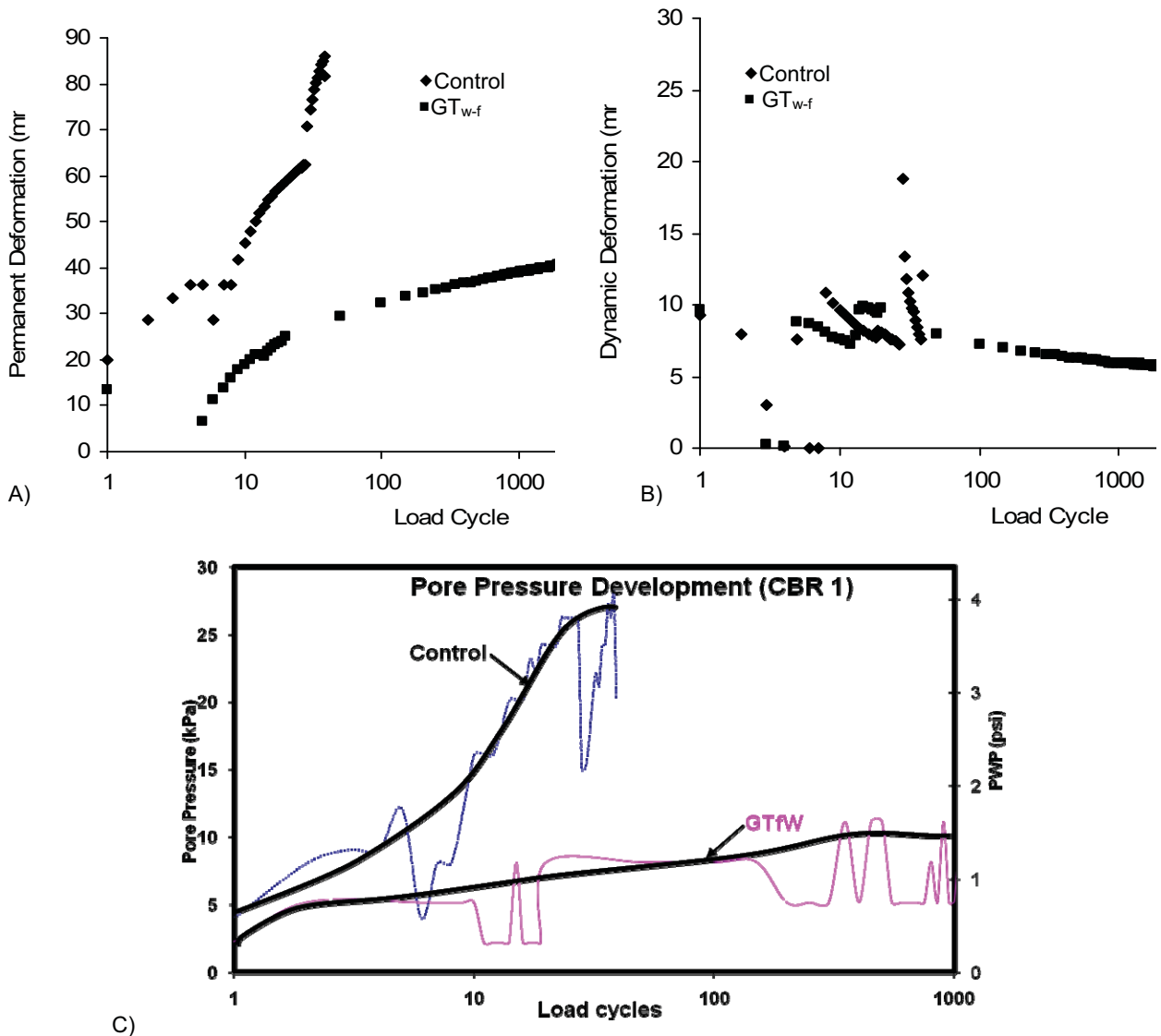


Figure 1. Representative Large Scale Box Test Results for control and a woven geotextile showing the load cycles versus a) Permanent Surface Deformation b) the dynamic deformation, and c) the excess pore pressure in the top of the subgrade

3. SOIL STRENGTH IN RELATION TO PORE WATER PRESSURE

The influence of pore water pressure on the strength of the soil can be computed from well established soil mechanics effective stress principles (e.g., Lambe and Whitman, 1969). Figure 2 shows a Mohr-Coulomb diagram for a normally-consolidated clay having an effective cohesion of zero and an effective friction angle of ϕ' . An element of the subgrade soil prior to roadway construction can be characterized by an initial state of stress with zero pore water pressure. This state of stress is represented by point i in Figure 2 having total and effective stresses given by $\sigma'_{1i} = \sigma_{1i}$ and $\sigma'_{3i} = \sigma_{3i}$. If this sample was sheared in an unconsolidated-undrained conventional triaxial compression test, it would result in an undrained shear strength given by S_{ui} , and with total and effective stresses as given in Figure 2 and where the additional subscript f denotes failure. The pore water pressure developed during undrained shear is given by u_{ti} and is equal to:

$$[1] \quad u_{ti} = \sigma'_{3i} - \sigma'_{3i-f}$$

Skempton's pore water pressure equation can be used to relate the excess pore water pressure, u_{ti} , to the increase in total stresses during triaxial loading:

$$[2] \quad u_{ti} = B\Delta\sigma_3 + A_f(\Delta\sigma_1 - \Delta\sigma_3)$$

where A_f denotes the pore water pressure parameter A at failure. For triaxial loading, $\Delta\sigma_3 = 0$ and equation 2 reduces to:

$$[3] \quad u_{ti} = A_f\Delta\sigma_1$$

Furthermore, in a triaxial test, $\Delta\sigma_1$ is equal to the diameter of the total stress Mohr's circle, which can be expressed in terms of the total major and minor principal stresses, which in turn is equal to two times the undrained shear strength:

$$[4] \quad \Delta\sigma_1 = \sigma_{1i-f} - \sigma_{3i} = 2S_{ui}$$

The effective stress equation can be used to relate the minor principal stresses to the excess pore water pressure:

$$[5] \quad \sigma'_{3i-f} = \sigma'_{3i} - u_{ti}$$

Substitution of equation 3 and 4 into 5 results in:

$$[6] \quad \sigma'_{3i-f} = \sigma'_{3i} - 2A_fS_{ui}$$

The undrained shear strength is by definition:

$$[7] \quad S_{ui} = \frac{\sigma'_{1i-f} - \sigma'_{3i-f}}{2}$$

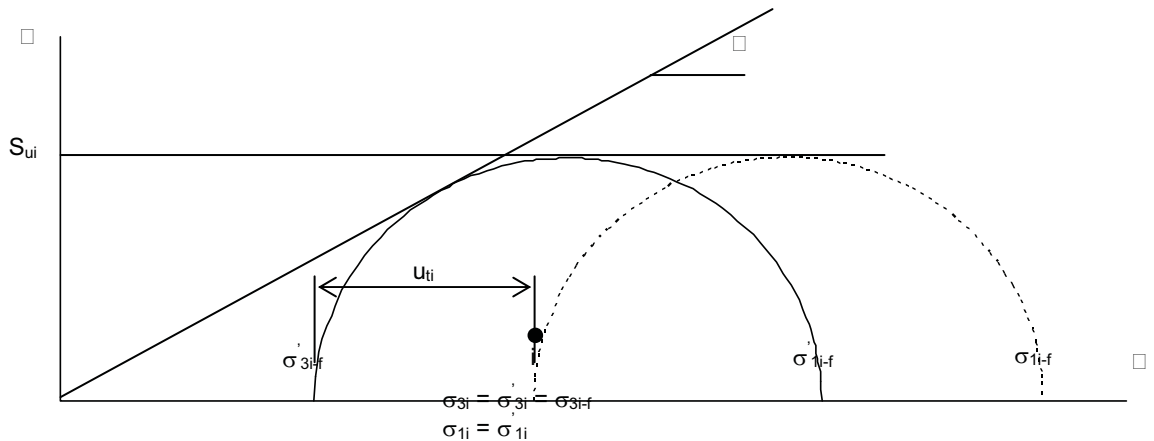


Figure 2. States of stress and undrained shear strength for pre-construction subgrade
The major and minor effective principal stresses at failure can be related to the friction angle by the equation:

$$[8] \quad \sigma'_{1i-f} = \sigma'_{3i-f} \tan^2(45 + \phi/2)$$

Substitution of equation 8 and 6 into 7 and solving for σ'_{3i} gives:

$$(9) \quad \sigma'_{3i} = S_{ui} \left[\frac{2}{\tan^2(45 + \phi/2) - 1} + 2A_f \right]$$

After roadway construction and trafficking, an excess pore water pressure (u_e) is developed, which is the excess pore water pressure in an unloaded state that develops after repeated trafficking. For the same element of subgrade as examined above, if the total stresses of the post-trafficked sample are unchanged, the effective stresses are reduced by u_e . This sample now has a state of stress given in Figure 3, with u_e given by:

$$(10) \quad u_e = \sigma'_{3i} - \sigma'_{3f}$$

If this sample is now sheared in an unconsolidated-undrained conventional triaxial compression test, lower undrained shear strength (S_{uf}) will result. By following the same procedure as detailed above, it can be shown:

$$(11) \quad \sigma'_{3f} = S_{uf} \left[\frac{2}{\tan^2(45 + \phi/2) - 1} + 2A_f \right]$$

Substitution of equations 9 and 11 into 10 results in:

$$(12) \quad u_e = (S_{ui} - S_{uf}) \left[\frac{2}{\tan^2(45 + \phi/2) - 1} + 2A_f \right]$$

Based on consolidated undrained triaxial tests with pore pressure measurements, the subgrade soil has an effective friction angle of 30 degrees and a typical value of A_f of 0.7. Thus, for this subgrade equation 12 reduces to:

$$(13) \quad u_e = 1.4(S_{ui} - S_{uf})$$

This overly simplified example illustrates the important role that build up of pore pressure from the repeated loading has on the undrained shear strength of the subgrade material. Actual performance is complicated by the facts that A_f for the soil may change with repeated loading and the excess pore pressure may dissipate if the repeated loading is spread out over time so that excess pore pressures can drain away.

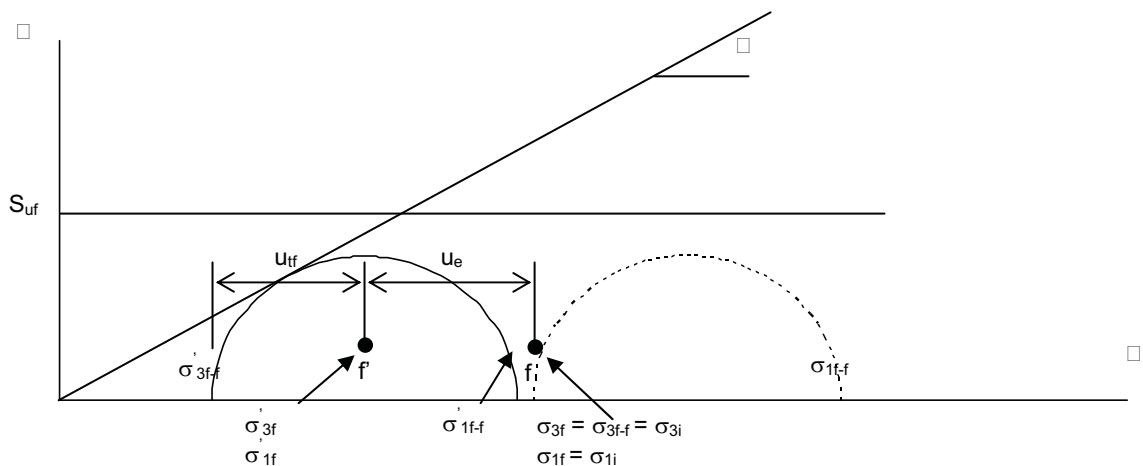


Figure 3. States of stress and undrained shear strength for post-construction and trafficking subgrade

4. ACCOUNTING FOR PORE WATER PRESSURE IN DESIGN

After construction, the subgrade had an undrained shear strength of 30 kPa (4.4 psi) as measured from a vane shear test. In the unreinforced test section, the excess pore water pressure is seen in Figure 1c to increase by an average value of approximately 28 kPa (4.0 psi). This reduces the effective stresses in the subgrade and results in a lower value

of undrained shear strength and stiffness. Using Equation 13, an increase in pore water pressure of 28 kPa results in an undrained shear strength of 10 kPa (1.4 psi).

Resilient modulus and permanent deformation testing on the subgrade material showed that the subgrade has an elastic modulus between 5.5 to 6.9 MPa (800 to 1000 psi) prior to testing. The pore-water pressure build-up in the subgrade layer of the unreinforced test section results in a reduction of both strength and stiffness of the subgrade. If the decrease in undrained shear strength is assumed to be proportional to the decrease in elastic modulus, then the material will have a new modulus of 1860 kPa (270 psi).

The authors used this lower subgrade modulus as an input value in a mechanistic design model for the subgrade (Perkins et al., 2008). The response model results in terms of dynamic deflection were found to match the observed value of approximately 8 mm shown in Figure 1b, while use of the initial modulus of the subgrade (0 pore water pressure) resulted in an overly stiff response with a dynamic deflection that was much less than the observed average value. Reinforced response model modules corresponding to compaction, traffic 1, traffic 2 and traffic 3 modules were created, where these modules were described by Perkins et al. (2004). The compaction module describes the increase in lateral confining stress in the base aggregate during the compaction of the aggregate. The traffic 1, 2 and 3 modules are used to define the build-up of lateral stress in the aggregate during traffic loading of the section. From the unreinforced and reinforced response models, the distribution of dynamic vertical strain with depth through the base aggregate and subgrade layers was determined and used in a damage model for rutting, as described in the paper by Perkins et al. (2008). For the reinforced test section, the excess pore water pressure was approximately 7 kPa (1.0 psi). Using the same approach described above, the elastic modulus of the subgrade for the reinforced test section was 4600 kPa (667 psi). Following guidelines established by Perkins et al. (2004), the cyclic elastic modulus of the geotextile in the machine and cross-machine directions and the material's Poisson's ratio was used to determine an equivalent isotropic elastic modulus of 790 MPa (115 ksi). Figure 4 shows the predicted results of the unreinforced and reinforced section as compared to the test results. The steps taken to account for the reduced excess pore water pressure in the reinforced test section as compared to the unreinforced section accounted for approximately 80 % of the reduced rutting. An additional 20 % is accounted for by the effects of the reinforcement. Overall, the predicted rutting using the reinforced model is greater than that seen in the reinforced test section but shows considerable improvement as compared to the unreinforced section and is regarded as a favorable and successful prediction.

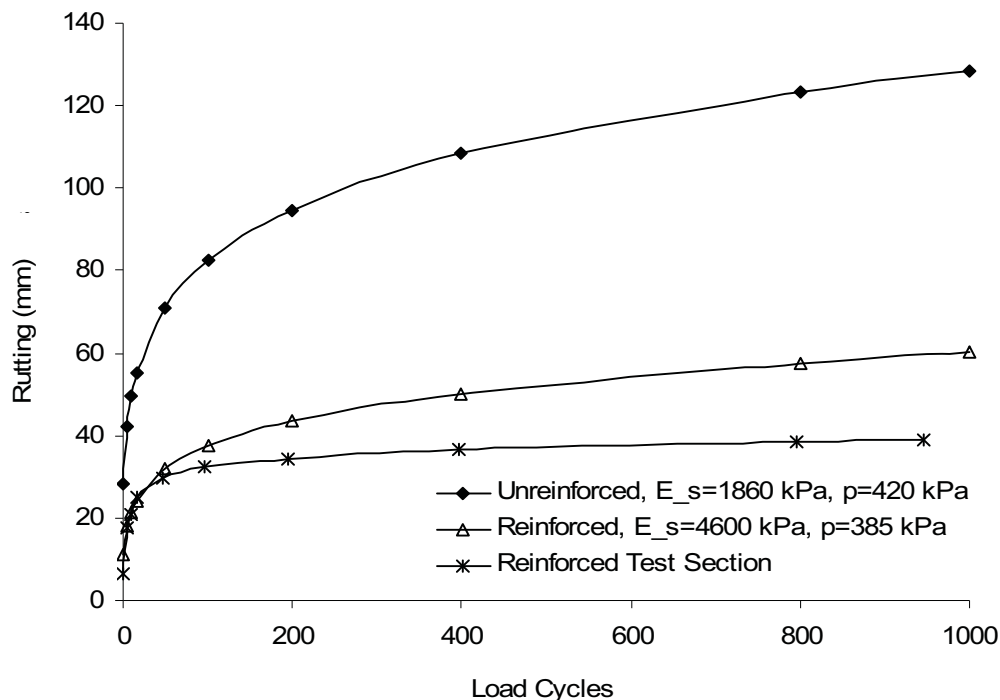


Figure 4. Unreinforced and Reinforced rutting predictions and comparisons

5. DEVELOPMENT OF DESIGN CHARTS WITH CONSIDERATION FOR PORE WATER PRESSURE

Traditional design charts can be modified to account for specific subgrade conditions to include the effect of pore water pressure build up during trafficking though the use of mechanistic-empirical design as discussed in the previous section. As an example, unreinforced design curves were developed for the silt type subgrade used in the example test section shown in Figure 1 (see Perkins et al., 2008 for complete details and input parameters for the mechanistic design model). The base line charts used for comparison were the design charts by Barenberg, 1975 and United States Forest, USFS, curves (Steward et al., 1977). Models of four cross sections having an aggregate thickness of 1000 mm, 760 mm, 500 mm, and 300 mm (40, 30, 20 and 12 in.) were created and analyzed. For simplicity, the stiffness value in the model is taken to be the subgrade resilient modulus at the end of trafficking when the pore water pressure build up is the greatest. Equation 13 was used to determine what u_e needed to be for each of the four model runs to gives an S_{ui} matching the traditional design curves for the S_{uf} used in the model. This results in values for u_e shown below in Table 1.

The four unreinforced models were analyzed by varying the subgrade resilient modulus until 75 mm (3 in.) of rut were developed in 1000 passes of the 45 kN (9000 lb) wheel load inflated to 550 kPa (80 psi). Figure 5 shows the design chart with values of subgrade CBR and resilient modulus plotted against the aggregate thickness for these four sections as compared to the original Barenberg design chart and the USFS design curve. In the evaluation of these cross-sections, the permanent deformation properties of the subgrade were varied as the resilient modulus varied. Principles contained in El-Basyouny et al. (2005) were used to adjust the subgrade permanent deformation properties. The difference in the subgrade CBR between the mechanistic-empirical model and the traditional design curves is due to the effect of pore water pressure build up during trafficking. The adopted approach was to assume that the initial subgrade CBR should lie on the traditional unreinforced design curves and that the difference between the final (model value) and initial (traditional design curve) undrained shear strength was due to the increase in pore water pressure during trafficking.

The authors are currently creating the reinforced design charts using both the data from the tests sections and the mechanistic-empirical model approach described previously in section 4. The result for the singular data point described in the previous section for a cross section with 12 inches of gravel is shown on Figure 1. Traffic loads on these sections were modeled identically to that for the unreinforced cross sections. Additional cross sections will be evaluated and the complete charts published in a future paper.

Table1: Initial and final shear strength and excess pore water pressure for unreinforced model cross-sections

Model Thickness (in)	Aggregate Thickness (in)	Initial Undrained Shear Strength, S_{ui} (kPa)	Final Undrained Shear Strength, S_{uf} (kPa)	Excess Pore Water Pressure, u_e (kPa)
40	40	6.80	6.08	1.01
30	30	14.70	10.53	5.84
20	20	26.30	17.83	11.86
12	12	55.00	39.43	21.80

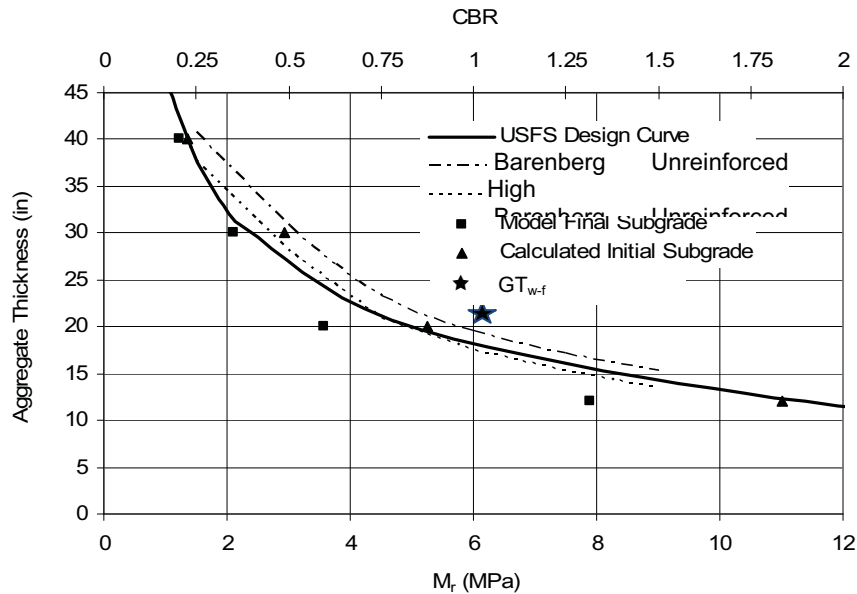


Figure 5: Model final subgrade CBR versus aggregate thickness with consideration for pore water pressure.

6. CONCLUSION

The laboratory test sections indicated that pore water pressure development played a significant role in the rutting behavior of the test sections. In the mechanistic-empirical modeling, pore water pressure development can be accounted for by adjusting the shear strength of the soil based on the effective stress principle of soil mechanics. Pore water pressure can be empirically included in design charts by matching unreinforced results to previously established design curves and then extending these results to reinforced sections using a reduced pore pressure development consistent with that observed in test sections. The mechanistic-empirical technique appears to work well for unpaved roads experiencing on the order of 1000 wheel passes for 75 mm of rutting, as long as the influence of pore water pressure is included in the analysis.

REFERENCES

- Barenberg, E.J., Hales, J., and Dowland, J. (1975). Evaluation of Soil-Aggregate Systems with MIRAFI Fabrics, UIIU-ENG-75-2020 Report for Celanese Fibers Marketing Company, University of Illinois, Urbana.
- Berg, R.B., Christopher, B. R. and Perkins, S., Geosynthetic Reinforcement of the Aggregate Base/Subbase Courses of Pavement Structures, prepared for American Association of Highway and Transportation Officials Committee 4E, Prepared by the Geosynthetic Materials Association, 2000, 176 p.
- Christopher, B.R., Berg, R.R., Perkins, S.W. (2001) Geosynthetic Reinforcements in Roadway Sections National Cooperative Highway Research Program, NCHRP Project 20-7, Task 112, FY2000, Transportation Research Board, National Academy Press, Washington, D.C., 2001.
- Christopher, B.R. and Lacina, B., "Roadway Subgrade Stabilization Study", Proceedings of GeoAmericas 2008, Cancun, Mexico, 2008, International Geosynthetic Society, pp. 1013–1021.
- Christopher, B.R. and Perkins, S.W. (2008) "Full Scale Testing of Geogrids to Evaluate Junction Strength Requirements for Reinforced Roadway Base Design," Proceedings of the Fourth European Geosynthetics Conference, Edinburgh, United Kingdom, International Geosynthetics Society.
- El-Basyouny, M.M., Witczak, M. and Kaloush, K. (2005), "Development of Permanent Deformation Models for the 2002 Design Guide", *Transportation Research Board 2005 Annual Meeting Preprint*, 23p.
- Giroud, J.P. and Noiray, L. (1981). Geotextile-Reinforced Unpaved Roads, Journal of the Geotechnical Engineering Division, American Society of Civil Engineers, Vol. 107, No GT 9, pp. 1233-1254.
- Giroud, J.P. and Han, J. (2004a). *Design Method for Geogrid-Reinforced Unpaved Roads: I Development of Design Method*, Journal of Geotechnical and GeoEnvironmental Engineering, Vol. 130, No. 8, pp. 775- 786.
- Holtz, R.D., Christopher, B.R. and Berg, R.R. (2008). *Geosynthetic Design and Construction Guidelines*, U.S. Department of Transportation, Federal Highway Administration, Washington DC, Report No. HI-95-038, 1995 (revised 1998 and 2008), 396 p.
- Lamb. T.W. and Whitman, R.V. (1969), Soil Mechanics, John Wiley and Sons, Inc.
- Perkins, S.W., Christopher, B.R., Cuelho, E.L., Eiksund, G.R., Hoff, I., Schwartz, C.W., Svanø, G., and Watn, A. (2004). *Development of Design Methods for Geosynthetic Reinforced Flexible Pavements*, U.S. Department of Transportation, Federal Highway Administration, Washington, DC, FHWA Report Reference Number DTFH61-01-X-00068, 263p.
- Perkins, S.W., Christopher, B.R. and Lacina, B. (2008). "Mechanistic-Empirical Design Method for Unpaved Roads Using Geosynthetics," Proceedings of the Fourth European Geosynthetics Conference, Edinburgh, United Kingdom, International Geosynthetics Society.
- Steward, J., Williamson, R. and Nohney, J. (1977), *Guidelines for Use of Fabrics in Construction and Maintenance of Low-Volume Roads*, USDA, Forest Service, FHWA-TS-78-205.